HHS Public Access

Author manuscript

Adv Healthc Mater. Author manuscript; available in PMC 2020 February 25.

Published in final edited form as:

Adv Healthc Mater. 2020 February ; 9(4): e1900750. doi:10.1002/adhm.201900750.

Second Generation Nanoporous Silicon Nitride Membranes for High Toxin Clearance and Small Format Hemodialysis

Kayli Hill,
Biomedical Engineering Department, University of Rochester, Rochester, NY 14627, USA

Samuel N. Walker,
Biomedical Engineering Department, University of Rochester, Rochester, NY 14627, USA

Alec Salminen,
Biomedical Engineering Department, University of Rochester, Rochester, NY 14627, USA

Hung L. Chung,
Biomedical Engineering Department, University of Rochester, Rochester, NY 14627, USA

Xunzhi Li,
Department of Chemical Engineering, University of Rochester, Rochester, NY 14627, USA

Bahie Ezzat,
Biomedical Engineering Department, University of Rochester, Rochester, NY 14627, USA

Joshua J. Miller,
SiMPore, Inc., 150 Lucius Gordon Drive, Suite 110, West Henrietta, Henrietta, NY 14586, USA

Jon-Paul S. DesOrmeaux,
SiMPore, Inc., 150 Lucius Gordon Drive, Suite 110, West Henrietta, Henrietta, NY 14586, USA

Jingkai Zhang,
The Institute of Optics, University of Rochester Rochester, NY 14627, USA

Andrew Hayden,

Prof. J. L. McGrath, james.mcgrath@rochester.edu; Prof. D. G. Johnson, dean.johnson@rochester.edu.

Author Contributions

K.H. and S.N.W. contributed equally to this work. K.H. assisted in data curation, investigation, formal analysis, review, and editing. S.N.W. assisted in data curation, investigation, and formal analysis. A.S. assisted in data curation, investigation, methodology, formal analysis, review, and editing. H.L.C. assisted in data curation, investigation, and methodology formal analysis. X.L. assisted in methodology. B.E. assisted in investigation. J.J.M. assisted in data curation, investigation, and methodology. J.-P.S.D assisted in investigation and methodology. J.Z. assisted in data curation and investigation. A.H. assisted in data curation and investigation. T.B. assisted in data curation and investigation. L.P. assisted in data curation and investigation. M.N.M. assisted in data curation and investigation. T.R.G. assisted in resources and funding acquisition. J.A.R. assisted in supervision, resources, and funding acquisition. J.T. assisted in consultation on experimental design. L.D. assisted in investigation, supervision, writing, and review. A.A.S. assisted in conceptualization, methodology, and resources. J.L.M. assisted in conceptualization, resources, supervision, funding acquisition, writing, review, and editing. D.G.J. assisted in conceptualization, resources, supervision, funding acquisition, data curation, investigation, writing, review, and editing.

Conflict of Interest

The authors declare the following potential conflict of interest with respect to the research, authorship, and/or publication of this article: J. L. McGrath, T. R. Gaborski, and J. A. Roussie declare a competing financial interest as cofounders and equity holders in SiMPore Inc., a commercial manufacturer of NPN and other silicon-based membrane materials.

Supporting Information

Supporting Information is available from the Wiley Online Library or from the author.

The ORCID identification number(s) for the author(s) of this article can be found under https://doi.org/10.1002/adhm.201900750.

SiMPore, Inc., 150 Lucius Gordon Drive, Suite 110, West Henrietta, Henrietta, NY 14586, USA

Tucker Burgin,
Biomedical Engineering Department, University of Rochester, Rochester, NY 14627, USA

Lindsay Piraino,
Biomedical Engineering Department, University of Rochester, Rochester, NY 14627, USA

Marina N. May,
Biomedical Engineering Department, University of Rochester, Rochester, NY 14627, USA

Thomas R. Gaborski,
Biomedical Engineering Department, Rochester Institute of Technology, Rochester, NY 14623, USA

James A. Roussie,
SiMPore, Inc., 150 Lucius Gordon Drive, Suite 110, West Henrietta, Henrietta, NY 14586, USA

Jeremy Taylor,
Department of Nephrology, University of Rochester, Rochester, NY 14627, USA

Louis DiVincenti Jr.,
Department of Comparative Medicine, University of Rochester, Rochester, NY 14627, USA

Alexander A. Shestopalov,
Department of Chemical Engineering, University of Rochester, Rochester, NY 14627, USA

James L. McGrath,
Biomedical Engineering Department, University of Rochester, Rochester, NY 14627, USA

Dean G. Johnson
Biomedical Engineering Department, University of Rochester, Rochester, NY 14627, USA

Abstract

Conventional hemodialysis (HD) uses floor-standing instruments and bulky dialysis cartridges containing ≈2 m^2 of 10 micrometer thick, tortuous-path membranes. Portable and wearable HD systems can improve outcomes for patients with end-stage renal disease by facilitating more frequent, longer dialysis at home, providing more physiological toxin clearance. Developing devices with these benefits requires highly efficient membranes to clear clinically relevant toxins in small formats. Here, the ability of ultrathin (<100 nm) silicon-nitride-based membranes to reduce the membrane area required to clear toxins by orders of magnitude is shown. Advanced fabrication methods are introduced that produce nanoporous silicon nitride membranes (NPN-O) that are two times stronger than the original nanoporous nitride materials (NPN) and feature pore sizes appropriate for middle-weight serum toxin removal. Single-pass benchtop studies with NPN-O (1.4 mm^2) demonstrate the extraordinary clearance potential of these membranes (10^5 mL min^{-1} m^{-2}), and their intrinsic hemocompatibility. Results of benchtop studies with nanomembranes, and 4 h dialysis of uremic rats, indicate that NPN-O can reduce the membrane area required for hemodialysis by two orders of magnitude, suggesting the performance and robustness needed to enable small-format hemodialysis, a milestone in the development of small-format hemodialysis systems.

Keywords

animal models; hemodialysis; nanomembranes

1. Introduction

There were more than 745 000 patients with end-stage renal disease (ESRD) in the US in 2017 with 124 500 new cases reported.[1] The standard of care for these patients is lifelong hemodialysis (HD) treatments at a frequency of three times per week with 63% of prevalent ESRD cases undergoing HD in 2016. There are a number of patient-related problems with the current approach; In-center thrice-weekly treatments have been linked with significantly increased risk of cardiovascular events and mortality due to the extralong interdialytic period.[2] Also, postdialysis recovery time can be twice as long as the treatment time, during which patients report feeling ill, lethargic, and depressed, preventing most patients from holding a full-time job.[3] More importantly, life expectancies for ESRD patients have improved little in the past two decades, with almost no change (<1 year increase) for those 50 years of age and older.[1]

In an effort to improve both health outcomes and quality of life for those on HD, research groups, including ours, are working on technologies for portable, wearable, or implantable HD.[4–9] Such devices would not only provide lifestyle benefits in the form of mobility and convenience, they could also improve treatment outcomes by enabling more frequent or continuous dialysis (keeping uremic toxin levels steady with consistent water-, electrolyte-, and acid/base-balance) that more closely replicates a functioning kidney. The best hope for a healthier future for ESRD patients, short of a replacement kidney, is the emergence of disruptive technologies in HD therapy. One example is the wearable artificial kidney, which has been developed for peritoneal dialysis (PD),[4,7] and for HD[7] using miniaturized pumps and controls along with a standard hemodialyzer cartridge. Notably, these wearable devices are still bulky, weighing as much as ten pounds, and have difficulty with microbubbles and clotting issues that plague clinical continuous renal replacement.[10] Efforts to create a bioartificial kidney for extracorporeal treatment[11] or implantation[9] are even more ambitious. Ultimately, such systems would include a plasma filter, followed by an active filter that uses cultured cells to further aid in toxin clearance. Versions without the active filtration component have shown some promise in canine models.[9]

Our group has previously developed a variety of ultrathin (≤50 nm) nanoporous silicon-based membranes and have established their value in improving the efficiency and precision of separations.[12–16] Strikingly, the membrane pore sizes can be tuned to match specific molecular separation goals.[17] We hypothesize that nanomembranes have the ability to reduce the format for hemodialysis by orders of magnitude because they are 100–1000 times thinner than conventional hemodialysis membranes. Hydraulic permeability for the nanomembranes has been measured to be 150 cc min^{-1} bar^{-1} cm^{-2} (2.5×10^{-7}–5×10^{-7} m s^{-1} Pa^{-1}).[12] Other silicon-based membranes, such as those used in the canine model, being thicker are therefore less diffusively efficient than our silicon-nitride membranes.[9] A major challenge when working with these membranes, however, is the brittle nature of ultrathin

silicon, which can result in sudden membrane failure above a critical pressure.[18] We have made significant improvements over the last decade in our ability to manufacture ultrathin membranes with high yield and to increase the amount of continuous membrane area. Our standard 5.4 mm × 5.4 mm chip formats featuring nanoporous silicon nitride (NPN)[19] membranes are now highly reliable in both fabrication and function. Work with larger area membrane chips, however, remains a challenge. For this reason, our first task in the current effort was to develop a stronger version of NPN that would allow for sustained pressures seen in a standard HD configuration.

We have previously reported bench top studies demonstrating the capacity of nanomembranes to clear urea and middle-weight proteins while retaining albumin without any degradation in clearance rates over at least 12 h.[20] We have also developed a simulation for continuous hemodialysis that predicts ultrathin membranes can maintain toxins at homeostatic levels in human blood with as little as 81 cm^2 of area.[21] In related work, we developed a stable, conformal ≈7 nm poly-ethylene glycol (PEG) coating for NPN that blocks protein binding without occluding pores.[22] Here, we build on these foundational studies by directly testing the hypothesis that nanomembranes can significantly reduce the amount of membrane area required for hemodialysis compared to conventional dialysis membranes. After presenting an improved version of NPN, herein called NPN-O, we conducted bench-top studies to characterize the new materials for clearance, molecular separations, and hemocompatibility. Finally, we demonstrate that hemodialysis with ultrathin membranes can reduce urea levels to near-normal after 4 h of dialysis in a uremic rat model, while conventional membranes used in these same devices, did not lower urea levels detectably.

2. Results and Discussion

2.1. Production Modifications to Enhance NPN Membrane Strength

We sought to improve the strength of NPN with a modest increase from its original thickness of 50 nm.[19] We achieved this by increasing the thickness of the pnc-Si hard mask with an oxidation step (Figure 1a; see the Experimental Section,NPN-O) that allowed for a longer etch and enabled thicker membranes. We found that the pores in pnc-Si shrank during oxidation, which can be appreciated in sieving curves that reveal cutoffs of ≈10 nm for 50 nm NPN-O compared to ≈35 nm for NPN at the same thickness (Figure 1b). The 75 nm and 100 nm NPN-O materials display similar cutoffs at ≈30 nm; however, the 100 nm sieving curve contains a “hump” extending out to 80 nm due to pore mergers during the extended etching through 100 nm of SiN. These elongated pores may also explain why 100 nm NPN-O is not significantly stronger than 75 nm NPN-O in burst pressure tests (Figure 1c). Given these sieving and burst pressure results, 75 nm NPN-O was selected as our best choice for hemodialysis. We note that because the etching process is applied to one side of the membrane, the resulting pores of NPN-O are slightly tapered with larger openings facing the ion plasma and smaller openings on the “backside” (Figure 1d). We chose to orient NPN-O membranes so that the backside was facing the blood/sample channel in our dialysis experiments to allow the smallest pore dimension to determine size selectivity and potentially reduce fouling. Future work may benefit from the ability to tune membrane pore

sizes to match specific molecular separation goals as permitted by our fabrication technique. Additionally, the standard semiconductor manufacturing process of the silicon is scalable, making this membrane format practical for widespread application.

2.2. Characterization of Solute Clearance by 75 nm NPN-O

We tested 75 nm NPN-O in benchtop studies employing 5.4 mm × 5.4 mm chips with a single 0.7 mm × 2 mm membrane window.[23] These were integrated into a silicone-based microfluidic device featuring a fluid channel on each side of the membrane (Figure 2a).[20] We measured the reduction in urea after a single pass over the membrane in the presence of a counter flow of buffer on the back side (at twice the rate, as this ratio of sample to dialysate flow was found to produce negligible transmembrane flow). Samples were drawn from a volume collected in a fraction collector (Model 2110, Bio-Rad, CA, USA) as previously described.[20]

We looked for evidence of membrane fouling by studying the time course of urea reduction in the presence of 100% serum (Figure 3a). After a 2 h transient period in which samples were only partially dialyzed, the single-pass urea clearance stabilized at ≈20%, independent of the use of a conformal PEG coating.[22] Paired *t*-tests ($n = 3$) determined there was no significant difference ($p > 0.05$) between urea fractional losses at 3, 4, and 5 h and one-way analysis of variance (ANOVA) showed there was no significant difference ($p > 0.05$) between PEG and non-PEG membranes regarding urea clearance. This result suggests that while native NPN-O likely adsorbs some protein from the solution,[22] this does not hinder small molecule passage. This result is also in agreement with a 23% reduction predicted by a computational model of the system at these flow rates[24] (Figure 2b; see Supporting Information). We performed further clearance studies with a two-membrane chip, which increases clearance and helps to accurately measure values for molecules with smaller diffusion coefficients like vitamin B12, cytochrome c and insulin. The results are shown in Figure 3b where it is shown that as the diffusion coefficient decreases, so does the clearance with FITC-insulin ($D = 8.2 \times 10^{-7}$ cm^2 s^{-1})[25] clearing more slowly than cytochrome c ($D = 1.63 \times 10^{-6}$ cm^2 s^{-1}).[26] Albumin clearance studies were also performed with nonporous membranes and the results showed that the outlet concentration matched that of the inlet indicating that no albumin was lost to the system (e.g., by adsorption).

Measuring clearance as a function of flow rate, we found that the area normalized urea clearance reached a maximum of ≈45 000 mL min^{-1} m^{-2} in the presence of 100% serum, and ≈60 000 mL min^{-1} m^{-2} in the absence of serum (Figure 4a). These values are orders of magnitude greater than the mass transfer coefficient, K_o, of conventional hemodialysis membranes (<1000 mL min^{-1} m^{-2} theoretical)[27] and the values reported for silicon slit-pore membranes (≈150 mL min^{-1} m^{-2}).[8]

We next examined the ability of 75 nm NPN-O to separate a middle-weight protein from bovine serum albumin (BSA) in a long-term, static experiment. Using cytochrome c (13 kDa) as a surrogate for the primary middle weight protein toxin β2-microglobulin in our single-pass system, (see Supporting Information). We reasoned that small variations in the rate of the transmission of differently sized proteins would be hard to discern in single-pass experiments, so we evaluated the loss through NPN-O after 24 h of microdialysis (Figure

4b). Results showed significant reduction in cytochrome c (≈55%) and less reduction for BSA (≈20%) over 24 h. As a positive control, KCL was almost completely lost to the large dialysate reservoir in the same experiments.

The microdialysis data indicate that untreated 75 nm NPN-O is significantly less permeable to albumin (63 kDa) then to a middle weight protein (13 kDa), meeting an important requirement for hemodialysis membranes. Although albumin is not substantially cleared by most hemodialysis treatments, clearance of some toxins, such as *p*-cresyl sulfate, would benefit from appropriate albumin clearance.[28,29] We hypothesized that PEG-coating would improve discrimination and possibly block albumin transmission completely. We previously showed that NPN functionalization with PEG1000 created a conformal ≈7 nm coating, which shrank pores by ≈14 nm in sieving tests.[22] Because our sieving curves for 75 nm NPN-O begin to show hindrance of solute transport at ≈20 nm, we reasoned that PEG-coating would significantly hinder the transport of molecules starting at ≈6 nm, which is roughly the hydrodynamic diameter of albumin[30] but >1.5 times larger than the hydrodynamic diameter of cytochrome c (3.6 nm).[31] Instead, there was no significant difference between BSA and cytochrome c reduction for the PEG-coated membranes, and a clear enhancement of BSA transmission over 24 h compared to nontreated membranes. These surprising results might be explained by the difference between convection and diffusion of solutes through PEG-coated pores. Water fills the space between the PEG polymer strands and permits solute transport by diffusion throughout the pore with little hindrance. By contrast, when pressurized flow is used, viscous flow converts the PEG layer to an extension of the no-slip region near the wall and effectively shrinks pores by the size of the PEG layer. In this way, the size-dependent hindrance seen in sieving curves might be a poor predictor of the hindrance by diffusion. Consistent with this, we previously showed that gas flow through NPN, which is a diffusive process,[32,33] was far less affected by a PEG coating than pressurized water flow.[22] The lower transmission of albumin in uncoated membranes can be explained by the fact that, lacking a PEG-coating in the presence of protein, silicon-based nanomembranes adsorb a monolayer of protein as thick as 3.5 nm.[15,16,22] Thus, a steric reduction in pore-sizes is expected for untreated membranes exposed to protein, which might hinder diffusion compared to expectations based on the pore sizes of the native material.[15]

2.3. Hemocompatibility of 75 nm NPN-O

In further bench-top experiments, we characterized the compatibility of 75 nm NPN-O with the constituents of whole blood. We first confirmed that a PEG coating dramatically reduced the number of cells that adhered to NPN-O membranes exposed to whole ovine blood in counter flow experiments (Figure 5a). While this result highlights the need for a nonstick coating on NPN-O, our albumin transmission results (Figure 4b) posed a dilemma and we decided to continue the studies with uncoated membranes while we developed a more comprehensive coating strategy. Fortunately, our studies revealed that native NPN-O membranes show little tendency to trigger immune activation (measured by C3a generation; Figure 5b) or coagulation (measured by thrombin-anti-thrombin complex (TAT) generation; Figure 5b) in blood. By contrast, diethyl-amino-ethyl cellulose, which has been used in hemodialysis membranes,[34] exhibited higher levels of TAT activation. Polysulfone (PSU)

also exhibited levels of TAT activation that are equivalent to the native NPN-O membranes. By these measures, native NPN-O membranes are hemocompatible and since PEG coating does not improve urea clearance (Figure 3a) we decided to move forward with uncoated membranes. We note that our studies were done in static incubation to avoid the dilution of signal that occurs with flow. Thus, while the results reveal intrinsic hemocompatibility for NPN-O, the potential activation of platelets via shear stress remain unknown.[35] Further studies are needed to determine if PEG-coating is important for hemocompatibility under flow.

2.4. Small Animal Model Hemodialysis

To test the ability of NPN-O to reduce toxins in vivo, we employed a uremic rat model and an extracorporeal circuit based on the experiment described by Yorimitsu et al.[36] In these experiments, Sprague-Dawley rats were fed an adenine-containing diet for two weeks to impair kidney function and to elevate serum urea concentration to more than two times the normal values,[36] then hemodialyzed with an extracorporeal circuit containing the test dialyzer (Figure 6a). We conducted the experiments with large area membrane chips featuring multiple membrane windows (Figure 6b) similar to those we have previously described.[37] Using two chips, we created a device with 110 mm^2 active membrane area. By contrast, Yorimitsu et al. used 4670 mm^2 of conventional hollow-fiber PSU dialysis membranes.[36]

Preparatory studies with the uremic animals demonstrated that nonporous membranes did not reduce urea levels after 4 h of dialysis (Figure 7a). These findings ensured that any reduction in urea in subsequent experiments was attributable to the diffusion into the dialysate. We measured vital signs and found a steady heart rate and a slight decrease in blood pressure (BP) over the 4 h treatment under anesthesia (Figure 7b). The decrease in BP over time was expected with anesthesia. We examined the membrane surface, after dialysis, by reflected light microscopy and found a region of cellular adhesion over ≈1.5 mm spans at both ends of the membrane (Figure 7c). This finding could be anticipated from our in vitro studies (Figure 5a) and underscores our continuing need for a nonstick coating that is compatible with large area nanomembranes.

Small-animal experiments with 75 nm NPN-O membranes reduced urea levels by 26% with 4 h of hemodialysis (Figure 8), while causing no detectable reduction in albumin. While a small amount of albumin leakage was expected based on our microdialysis studies (Figure 4b) and some albumin leakage would have been acceptable,[28] the presence of flow in these 4 h hemodialysis experiments limits the interaction time between solutes and membranes and longer dialysis times might be required to detect albumin clearance.

A single experiment with our standard 50 nm NPN[19] showed slightly better clearance than 75 nm NPN O, however, it spontaneously fractured at 3.5 h. By contrast, all experiments started with 75 nm NPN-O remained intact over the 4 h HD experiments. These mechanical stability differences validate our efforts to create stronger NPN membranes.

In contrast to results with NPN and NPN-O membranes, conventional dialysis materials used in the same device did not lead to a measurable reduction in urea clearance. The

conventional membranes actually had ≈2 times more area exposed to blood and dialysate when integrated into the devices, but still showed no detectable clearance. Yorimitsu et al. saw a ≈25% reduction in urea over 2 h in the same rat model using 4670 mm^2 of polysulfone PSU hemodialysis membrane.[36] This was 20 times the area of PSU that we used in our small-animal experiments, therefore it is not surprising that we saw no reduction in urea after 4 h. Note that the comparison to Yorimitsu et al.[36] directly supports our hypothesis that nanomembranes can reduce the amount of membrane required for hemodialysis by orders of magnitude. Even these nonoptimized experiments required ≈1/20 the membrane area to achieve a similar clearance as seen in Yorimitsu et al.[36] Additional performance improvements can be expected by adjusting flow rates to optimize clearance and achieving a nonstick coating to eliminate cell adhesion at the device inlet and outlet. Increasing the membrane area by ≈40% would further improve clearance in the same footprint of the device and we should achieve HD doses of $Kt/V = 1.8$ in the rat dialysis model in 4 h, above the clinical target of $Kt/V = 1.2$. While our ultimate goal is continuous hemodialysis in a human, hitting this preclinical benchmark in a small animal model for 4 h HD sessions are key milestones on the development path to this goal. The fabrication advancement to increase the strength of the nanoporous silicon nitride membranes was crucial to the success of this study.

3. Conclusions

The benefits of frequent hemodialysis are well-documented.[3] Yet less than 0.5% of incident ESRD patients elect home hemodialysis (in the US in 2017), where more frequent treatment is feasible, citing the need for large, complex equipment, the appointment of caretakers, and self-cannulation as reasons to continue with the less beneficial thrice-weekly therapies.[38–41] Only a revolutionary change in therapy that improves longevity, lifestyle, and daily well-being will disrupt the current regime of hemodialysis therapy. Our work suggests that ultrathin dialysis membranes may represent one of the disruptive technologies needed for this revolution. For NPN-O membrane technology, challenges still remain. First, we need to develop nonfouling coating strategies that can be applied to large-area membranes. This will also require the use of human blood in future hemocompatibility studies. Even with these developments, a highly efficient membrane is only one of the technologies needed for a continuously wearable hemodialysis therapy. To reduce both the extracorporeal volume and the footprint so that wearing a device is comfortable and inconspicuous, other technologies such as on-device anticoagulation, absorption-based toxin removal, and vascular access, also need to be developed and integrated with the membrane.

4. Experimental Section

NPN-O Membrane Fabrication:

NPN membranes were fabricated as previously described[19] and NPN-O membranes were manufactured with modifications to this process (Figure 1a). Silicon and silicon dioxide were deposited on wafers coated with 50, 75, or 100 nm of silicon nitride and converted to 32 nm or 40 nm porous-nanocrystalline silicon (pnc-Si) by a rapid thermal anneal. Material properties (e.g., thickness) of the deposited silicon and silicon nitride, along with the anneal

parameters, controlled the pore size and density.[17] The capping oxide layer was etched away to reveal the pnc-Si pore-transfer mask. The pnc-Si was then oxidized to make it thicker and more resistive as an etch mask. Pores were then transferred to the underlying SiN through a reactive ion etch (RIE) which also consumed the mask. For NPN-O, a thermal oxidation step was carried out prior to the pore transfer step, by treatment at 1000 °C for 210 min in a tube furnace and an oxygen atmosphere (Bruce Technologies Inc., MA, USA). This thermal oxidation step converted the porous silicon to porous silicon oxide for NPN-O fabrication.

The outer dimensions of the chip and the membrane geometry were defined using conventional photolithography and RIE patterning, followed by through-wafer etching with ethylenediamine pyrocatechol (EDP; Transene Inc.) to expose the underside of the membranes, thus making both sides fluidically accessible. SEM images of the membrane in cross section were used to determine their thickness. A custom MATLAB program was used to analyze STEM images of membranes to determine pore statistics.[13]

Single-Pass Bench-Top Dialysis:

Devices were constructed with either a single-membrane chip or a two-membrane chip enclosed with three layers of silicone gasket material; one of the layers (300 μm thick) acts as a collar for the chip; the other two (100 μm thick) contain fluid channels. The gaskets and chip were bonded together via a UV/ozone bonding process. An upper layer of PDMS (which holds the inlet/outlet tubing) and a #1.5 coverslip slide (to provide stability from underneath) were bonded via two-sided adhesive tape (120 μm thick) patterned with fluidic channels. The analytes flowed through the upper channels into the trench etched into the silicon chip and came in contact with the nanoporous membrane. Dialysate (clean phosphate-buffered saline (PBS)) flowed in the opposite direction in the lower channel and contacted the membrane on the flat side of the chip.

The analyte fluid (e.g., 5×10^{-3} M urea in 100% fetal bovine serum (FBS)) was passed over the top side (trench) of the membrane (either PEG-coated or bare) while PBS (dialysate) was passed on the underside (flat surface of the chip). The dialysate and analyte were pumped in opposite directions to increase the concentration gradient along the fluid channels. For the transient experiments, the flow rates for the analyte and dialysate were set to 1 and 2 μL min^{-1} respectively. The dialysate was run at twice the analyte rate to reduce transmembrane pressure and ultrafiltration while mimicking clinical dialysis. The 1:2 ratio of analyte flow rate to dialysate flow rate was determined optimal for reducing ultrafiltration effects by passing a volume of fluid over the membrane at a known flow rate and for a defined amount of time. For the clearance versus flow-rate experiments, a range of flow rates was used for the analyte flow (10, 50, 100, 1000, 2000, and 4000 μL min^{-1}) with the dialysate always twice the analyte. By measuring the final volume and comparing it to the expected volume, the ultrafiltration could be determined. This was done for a range of analyte to dialysate flow rate ratios (1:1, 3:4, 1:2) and the 1:2 ratio was least affected by ultrafiltration. The setup used syringe pumps (NE1000, New Era Pump Systems, Inc., NY, USA) to deliver the fluids and a fraction collector, allowing for fully automated collection of samples over the entirety of the experiment, giving the user flexibility in designing long experiments with many sample

collections over a variety of flow rates. For the current research, samples were collected every hour for 6 h. Samples were analyzed using a colorimetric assay (BioVision, California, USA). After performing the colorimetric urea assay, the data was normalized to the second hour time point. This was done because nondialyzed priming fluid, analyte, remained in the tubing after priming the device with analyte until the third hour point.

The urea clearance rate, k^* (normalized to membrane area), was calculated using the fractional loss

$$k^* = (f\,Q)/A_{\mathrm{m}} \tag{1}$$

where f is the fractional loss, Q is the analyte flow rate, and A_{m} is the membrane area. To optimize clearance, the same setup and devices were used as in the previous experiment with the flow rates increased. Dialysate was always run at two times the analyte flow rate. The same volume was pushed over the membrane for every flow rate, meaning the duration of the experiments changed but the collected volume did not. Collected fluid volumes were monitored to ensure no false clearance values due to backflow.

As the flow rates of the analyte and dialysate were increased, the value of the area-normalized single-pass clearance, k^*, approached the mass transfer coefficient for the dialyzer K_{o}.[42,43] For the dialyzer, at 4 mL min^{-1}, $K_{\mathrm{o}} = k^* \approx 45000$ mL min^{-1} m^{-2}, or $\approx 7.5 \times 10^2$ cm s^{-1}. Commercial high-flux dialyzers, with ≈ 1.8 m^2 surface area, had a K_{o} of ≈ 560 mL min^{-1} m^{-2}, two orders of magnitude smaller than the K_{o} of the nanoporous membranes.[44]

PEG Coatings:

The native surface of the NPN-O membranes was first deposited with NHS-Diazirine through vacuum phase reaction[45] and further grafted with PEG1000 (#B22134, Alpha Aesar, MA, USA) largely as described previously.[22] The PEG reaction temperature (75 °C) was increased for the 5.4 mm × 5.4 mm chips, because it was found that the high temperature increased the solubility of the PEG and helped the reaction on the NPN surface.

Microdialysis Studies:

To examine the separation of proteins with NPN-O, a SepCon spin cup[19] was modified by drilling a small hole in the bottom of the lower retaining bucket. Analyte (50 μL) was loaded on top of the membrane and the assembly was suspended in a PBS-filled beaker that was placed on a magnetic stirrer. The added hole in the bottom of the spin cup was done to promote the removal of molecules that had diffused across into the bulk fluid in the beaker. The analyte was composed of 1 mg mL^{-1} BSA or 1 mg mL^{-1} cytochrome c, or 3×10^{-9} M KCl. The fluid level in the cup was matched to the fluid line of PBS in the beaker to ensure no net-hydrostatic pressure was acting on the diffusing fluid, and analyte was covered to prevent evaporation. Dialysis occurred at 4 °C for 24 h. The fluid remaining in the column was sampled after 24 h and analyzed. Fluid levels were inspected to confirm that evaporation or flow did not occur. Nonporous membrane controls were used as a baseline for losses due to protein adsorption to plastic. Cytochrome c concentrations were measured with a colorimetric assay. Albumin concentrations were measured via colorimetric assay

(BioVision, California, USA). KCl concentrations were measured with a conductance meter (Con 6, Oakton, Melbourne, Australia). All p values were found using paired t tests ($n = 3$). Each experiment was repeated ($n = 3$) with nonporous membrane chips (with the membrane material on the surface). The loss of analyte from these experiments could not have been from diffusion and were assumed to be adsorption onto the surfaces of the membrane and the spin cups. These values were subtracted from the raw experimental data.

Hemocompatibility—Cell Adhesion:

Cellular adhesion with whole ovine blood (Innovative Research, MI, USA) in a counter-flow device was compared between untreated and PEG-coated membranes. In 5.4 mm single-membrane chips, ovine blood was flowed at 3 μL min^{-1} though the 3 mm × 1 mm channels with PBS flowed at the same rate but in the opposite direction for 4 h. The chips were prewetted with PBS and rinsed following flow. The membrane surfaces were fixed with 4% paraformaldehyde for >10 min and rinsed again. One set of three chips was untreated, bare, while another group of three was coated with PEG. Using an optical microscope, ImageJ (imagej.nih.gov, Public Domain) for B&W thresholding, and a custom processing MATLAB tool developed by the lab, the percent of area covered by cellular material was measured.

Hemocompatibility—Substrate Coagulation and Complement Activation:

The concentration of TAT and C3a complement measured via ELISA kit (Abcam, MA, USA) was used as indicators of coagulation and immune activation, respectively. A hole-punched PDMS block was placed on top of the substrate to define a circular area (10 mm diameter) for sample incubation. Platelet rich plasma (PRP) and whole human blood was used as the samples for the TAT and C3a ELISA, respectively. 200 μL of sample was placed on the substrate and kept in the incubator (37 °C; 5% CO_2; 80% relative humidity) for 2 h before the sample retrieval for ELISA. PDMS was one of the substrates tested, and the corresponding TAT and C3a measurement were used for background subtraction. Blood with 10×10^{-9} M fMLP was used as the positive control for C3a ELISA. 40×10^{-6} M ADP in PRP was used as the positive control for TAT. From images of activated platelets, it was determined that all the adhered platelets were activated, and most activated platelets exhibited similar level of CD62P expression (<twofold difference). The fluorescence intensities of all activated platelets were summed in each image for quantitative analysis. Significant differences were seen in all pairwise comparisons (ANOVA).

Hemocompatibility—Platelet Adhesion and Activation:

A PDMS block with rectangular grooves (1 mm × 1 mm × 2 cm) and hole-punched inlet/outlet at either end was placed on top of the substrate to define the microchannels for platelet incubation. 20 μL of PRP was pipetted into each microchannel and kept in the incubator for 2 h. The samples were then inverted to allow the loose platelets to settle onto the channel roof for 30 min. The samples were washed with PBS, fixed via 4% paraformaldehyde (20 min, RT), blocked with BSA (20 mg mL^{-1}, 1 h at RT), and incubated with primary antibodies overnight at 4 °C. The primary antibodies used were 20 μg mL^{-1} anti-CD41 (platelet adhesion) and 20 μg mL^{-1} anti-CD62P (platelet activation). After 24 h, the samples were washed with PBS and incubated with secondary antibodies (100 μg mL^{-1} of AF488 goat anti-mouse and 100 μg mL^{-1} AF568 goat anti-rabbit) for 1 h at RT. Lastly, the samples

were washed with deionized water and let dry before imaging. PRP with 40×10^{-6} M ADP (Bio/Data Corp, PA, USA) was used as the positive control for platelet activation. All reagents were purchased from Abcam (MA, USA) unless mentioned otherwise. The fluorescence images were analyzed using custom-written MATLAB routines. The background intensity was used as the threshold to segment the image into regions with platelets and regions without. The combined fluorescence intensity of the platelet regions in each image was used for the statistical analysis.

Hemocompatibility—Small Animal Model Dialysis:

All animal procedures were approved by and were conducted according to the guidelines of the University of Rochester's Vivarium and Committee on Animal Resources. All animals were housed and cared for in the Vivarium of the Univ. of Rochester School of Medicine & Dentistry. Methods of euthanasia that were used were consistent with the recommendations of the Panel on Euthanasia of the American Veterinary Medical Association.

Multichannel devices were constructed by incorporating fluidic components formed in polydimethylsiloxane (PDMS) with two 22 mm × 24 mm membrane chips with 10 parallel microfluidic channels.[20] The chips were clamped between two acrylic plates for fixation with two PDMS gaskets on each side of the chips containing the fluidics. The PDMS gaskets in direct contact with the plates have channels that distribute fluid into two chips with equal pathway length, and the PDMS gaskets that contact the chip have punched holes that allow fluid to flow through the inlet and outlet channels.

Sprague-Dawley rats with implanted femoral vein, femoral artery, and carotid artery catheters were obtained from Envigo (MA, USA). All rats were housed singly to prevent cage-mates from manipulating the catheters since any failure of these catheters would result in a sudden death in the animal. Uremia was induced in rats with a 0.75% adenine-containing pelleted diet that was commercially prepared by Envigo to be nutritionally complete for rats.

After 2–3 weeks on the adenine-containing diet, the animals were anesthetized with isoflurane, and underwent hemodialysis for up to 4 h under anesthesia. Four paradigms were tested in replicates of short-term (4 h) treatments with sham dialysis, commercial hydrophilic membranes of either PSU or cellulose triacetate (CTA), and NPN membranes. PSU and CTA were both materials traditionally used in clinical dialysis and were used here for comparison and PSU was the material used by Yorimitsu et al.[36] Sham dialysis was conducted using nonporous nitride chips, which have the same channels in the chip surface as the nanoporous chips, without having the pores etched through the nitride membrane. Commercial membrane material was used in the same device in place of the NPN membranes by placing rectangular sheets of hydrophilic filter paper, 30 kDa PSU and 20 kDa CTA (Sartorious Stedim North America, NY, USA).

Up to 0.25 mL of blood was obtained from the femoral vein catheter once weekly to monitor the urea levels during induction of the kidney failure model. Every 60 min during dialysis, small blood samples (≈0.5 mL) were drawn upstream of the dialyzer (which was connected to the rat's vascular system through femoral artery and vein catheters). Thus, the urea levels

measured by the blood panel represented the blood urea level of the animal, not the urea in the blood exiting the dialysis device.

Animals were induced with isoflurane 2% to 4% in a chamber, and then maintained in a light surgical plane of anesthesia with isoflurane via nose cone at 1% to 3% for the duration of the procedure. Following induction of anesthesia, the animal received 100U heparin IV through an intravenous catheter. The tubing was primed with heparinized saline. Invasive blood pressure monitoring via the indwelling carotid artery catheter allowed monitoring the health of the animal throughout the experiment. The blood pressure and pulse readings were well within expected values. (BP ≈ 115/90, HR = ≈ 310 bpm).[46] While monitoring, the dialysis device was hooked into the vasculature, first to the artery, to fill the system with blood and remove the saline that was preloaded in the dialyzer. The output of the dialyzer was connected to the femoral vein catheter, completing the fluidic circuit. Without assistance of the blood pump the pressure of the vasculature pushed blood through the dialyzer at a rate of ≈1 mL min^{-1}, preventing stagnation in the extracorporeal circuit. A pump was used during HD to maintain consistent flow across the device. The dialysate bag (lactated ringers) was hung and connected to the basal side of the membranes. In preliminary experiments, rats were hemodialyzed for 30 min to test device performance and allow refinements. Midway through the 4 h experiments, an additional 100U heparin IV was administered.

All of the experiments used the setup shown in Figure 6a. A mini peristaltic pump (73160–31, Cole-Parmer, IL, USA) was used to pull blood from the femoral artery catheter through a pin-port (Instech Laboratories Inc., PA, USA) placed by Envigo (MA, USA). The blood then flowed through the tubing to the top layer of the dialysis device, flowing into the etched channels on both filter chips then back to the animal via the pin-ported femoral vein. Simultaneously, lactated Ringer's solution (as the dialysate) flowed from a drip bag across the flat side of the filter chips. There was a significant amount of breakage in the 50 nm NPN nanomembranes and an analysis of the system pressure and burst pressure of the membranes was performed.[37] The 4 h dialysis experiment was repeated with the 75 nm NPN-O nanomembranes with much better device survival. In the comparisons to commercial membranes, the conventional sheet membranes were bonded to a membrane-less chip with the same format as NPN/NPN-O with the polymer membranes free to dialyze across the entire 10 mm × 12 mm central region without occlusion from the intervening silicon supports.

Supplementary Material

Refer to Web version on PubMed Central for supplementary material.

Acknowledgements

The authors disclosed receipt of the financial support for the research, authorship, and/or publication of this article. This study was funded by NIH/National Institute of Diabetes and Digestive and Kidney Diseases K25 DK106503-01A1 to D.G.J., NIH/National Heart, Lung, and Blood Institute R21 EB021026 to J.L.M., National Science Foundation IIP1660177 to T.R.G. and J.A.R., and Fresenius Medical Care Inc. to D.G.J.

References

[1]. United States Renal Data System- 2019 USRDS Annual Data Report: Epidemiology of Kidney Disease in the United States, National Institutes of Health, National Institute of Diabetes and Digestive and Kidney Diseases, Bethesda, MD 2019.

[2]. Foley RN, Gilbertson DT, Murray T, Collins AJ, N. Engl. J. Med 2011, 365, 1099. [PubMed: 21992122]

[3]. Culleton BF, Walsh M, Klarenbach SW, Mortis G, Scott-Douglas N, Quinn RR, Tonelli M, Donnelly S, Friedrich MG, Kumar A, Mahallati H, Hemmelgarn BR, Manns BJ, JAMA, J. Am. Med. Assoc 2007, 298, 1291.

[4]. Lee DBN, Roberts M, World Congress on Medical Physics and Biomedical Engineering, September 7–12, 2009, Munich, Germany (Eds: Dössel O, Schlegel WC), Springer, Berlin 2009, pp. 104–107.

[5]. Gura V, Macy AS, Beizai M, Ezon C, Golper TA, Clin. J. Am. Soc. Nephrol 2009, 4, 1441. [PubMed: 19696219]

[6]. Wester M, van Gelder MK, Joles JA, Simonis F, Hazenbrink DHM, van Berkel TWM, Vaessen KRD, Boer WH, Verhaar MC, Gerritsen KGF, Am. J. Physiol 2018, 315, F1385.

[7]. Bazaev NA, Dorofeeva NI, Zhilo NM, Streltsov EV, Int. J. Artif. Organs 2017, 0, 1877.

[8]. Kim S, Feinberg B, Kant R, Chui B, Goldman K, Park J, Moses W, Blaha C, Iqbal Z, Chow C, Wright N, Fissell WH, Zydney A, Roy S, PLoS One 2016, 11, e0159526. [PubMed: 27438878]

[9]. Kensinger C, Karp S, Kant R, Chui BW, Goldman K, Yeager T, Gould ER, Buck A, Laneve DC, Groszek JJ, Roy S, Fissell WH, ASAIO J. 2016, 62, 491. [PubMed: 26978710]

[10]. Davenport A, Pediatr. Nephrol 2015, 30, 2053. [PubMed: 25330876]

[11]. Humes HD, Buffington D, Westover AJ, Roy S, Fissell WH, Pediatr. Nephrol 2014, 29, 343. [PubMed: 23619508]

[12]. DesOrmeaux JPS, Winans JD, Wayson SE, Gaborski TR, Khire TS, Striemer CC, McGrath JL, Nanoscale 2014, 6, 10798. [PubMed: 25105590]

[13]. Gaborski TR, Snyder JL, Striemer CC, Fang DZ, Hoffman M, Fauchet PM, McGrath JL, ACS Nano 2010, 4, 6973. [PubMed: 21043434]

[14]. Smith KJP, Winans J, McGrath J, Ultrathin Membrane Fouling Mechanism Transitions in Dead-End Filtration of Protein, ASME, New York 2016.

[15]. Snyder JL, Clark A, Fang DZ, Gaborski TR, Striemer CC, Fauchet PM, McGrath JL, J. Membr. Sci 2011, 369, 119.

[16]. Striemer CC, Gaborski TR, McGrath JL, Fauchet PM, Nature 2007, 445, 749. [PubMed: 17301789]

[17]. Fang DZ, Striemer CC, Gaborski TR, McGrath JL, Fauchet PM, J. Phys.: Condens. Matter 2010, 22, 454134. [PubMed: 21339620]

[18]. Gillmer SR, Fang DZ, Wayson SE, Winans JD, Abdolrahim N, DesOrmeaux J-PS, Getpreecharsawas J, Ellis JD, Fauchet PM, McGrath JL, Thin Solid Films 2017, 631, 152.

[19]. DesOrmeaux JPS, Winans JD, Wayson SE, Gaborski TR, Khire TS, Striemer CC, McGrath JL, Nanoscale 2014, 6, 10798. [PubMed: 25105590]

[20]. Johnson DG, Khire TS, Lyubarskaya YL, Smith KJP, DesOrmeaux J-PS, Taylor JG, Gaborski TR, Shestopalov AA, Striemer CC, McGrath JL, Adv. Chronic Kidney Dis 2013, 20, 508. [PubMed: 24206603]

[21]. Burgin T, Johnson D, Chung H, Clark A, McGrath J, Membranes 2015, 6, 6.

[22]. Li X, Johnson D, Ma W, Chung H, Getpreecharsawas J, McGrath JL, Shestopalov AA, Chem. Mater 2017, 29, 2294. [PubMed: 29651199]

[23]. Mossu A, Rosito M, Khire T, Chung HH, Nishihara H, Gruber I, Luke E, Dehouck L, Sallusto F, Gosselet F, McGrath JL, Engelhardt B, Cereb J. Blood Flow Metab. 2018, 39, 395.

[24]. Salminen A, Hill K, Henry Chung L, James McGrath L, Johnson DG, Conf. Proc.: Annual Int. Conf. of the IEEE Engineering in Med. and Biology Society. IEEE Engineering in Medicine and Biology Society. Annual Conf 2018, p. 5814.

[25]. Sober HA, Company CR, Harte RA, Sober EK, CRC Hand-book of Biochemistry: Selected Data for Molecular Biology, Chemical Rubber Company, Boca Raton, FL 1968.

[26]. Kontturi AK, Kontturi K, Niinikoski P, Savonen A, Vuoristo M, Acta Chem. Scand 1992, 46, 348. [PubMed: 1325179]

[27]. Daugirdas JT, Blake P, Ing TS, Blagg C, Dial. Transplant 2007, 36, 322.

[28]. Liabeuf S, Barreto DV, Barreto FC, Meert N, Glorieux G, Schepers E, Temmar M, Choukroun G, Vanholder R, Massy ZA, Nephrol., Dial., Transplant 2010, 25, 1183. [PubMed: 19914995]

[29]. Burgin T, Johnson D, Chung H, Clark A, McGrath J, ASME 2016 14th Int. Conf. on Nanochannels, Microchannels, and Minichannels, ASME, New York 2016.

[30]. Armstrong JK, Wenby RB, Meiselman HJ, Fisher TC, Biophys. J 2004, 87, 4259. [PubMed: 15361408]

[31]. Morar AS, Olteanu A, Young GB, Pielak GJ, Protein Sci. 2001, 10, 2195. [PubMed: 11604526]

[32]. Kavalenka MN, Striemer CC, Fang DZ, Gaborski TR, McGrath JL, Fauchet PM, Nanotechnology 2012, 23, 145706. [PubMed: 22433182]

[33]. Elwenspoek M, Jansen HV, Silicon Micromachining, Cambridge University Press, Cambridge 2004.

[34]. Ward RA, Schmidt B, Gurland HJ, Nephrol., Dial., Transplant 1993, 8, 1140. [PubMed: 8272230]

[35]. Sanak M, Jakiela B, Wegrzyn W, Bull. Pol. Acad. Sci.: Tech. Sci 2010, 58, 317.

[36]. Yorimitsu D, Satoh M, Koremoto M, Haruna Y, Nagasu H, Kuwabara A, Sasaki T, Kashihara N, Ther. Apheresis Dial 2012, 16, 566.

[37]. Johnson DG, Pan S, Hayden A, McGrath JL, 38th Annual Int. Conf. of the IEEE Engineering in Medicine and Biology Society, IEEE, Piscataway, NJ 2016, pp. 1955–1958.

[38]. Yau M, Carver M, Alvarez L, Block GA, Chertow GM, Hemodialysis Int. 2016, 20, 235.

[39]. Metzger S, Nephrol. Nurs. J 2016, 43, 251. [PubMed: 27501632]

[40]. Hanson CS, Chapman JR, Craig JC, Harris DC, Kairaitis LK, Nicdao M, Mikaheal M, Tong A, Nephrology 2017, 22, 631. [PubMed: 27253517]

[41]. Firanek CA, Garza S, Gellens ME, Lattrel K, Mancini A, Robar A, Todd LB, Sloand JA, Nephrol. Nurs. J 2016, 43, 195. [PubMed: 27501628]

[42]. Ouseph R, Ward RA, Am. J. Kidney Dis 2001, 37, 316. [PubMed: 11157372]

[43]. Leypoldt JK, Cheung AK, Agodoa LY, Daugirdas JT, Greene T, Keshaviah PR, Beck GJ, Kidney Int. 1997, 51, 2013. [PubMed: 9186896]

[44]. Hootkins R, Dial. Transplant 2011, 40, 392.

[45]. Li X, Ma W, Shestopalov AA, Langmuir 2016, 32, 11386. [PubMed: 27759398]

[46]. Shimoyama M, De Pons J, Hayman GT, Laulederkind SJF, Liu W, Nigam R, Petri V, Smith JR, Tutaj M, Wang S-J, Worthey E, Dwinell M, Jacob H, Nucleic Acids Res. 2015, 43, D743. [PubMed: 25355511]

[47]. Cussler EL, Diffusion: Mass Transfer in Fluid Systems, 3rd ed, Cambridge University Press, Cambridge 2009.

[48]. Collins MC, Ramírez W, J. Phys. Chem 1979, 83, 2294.

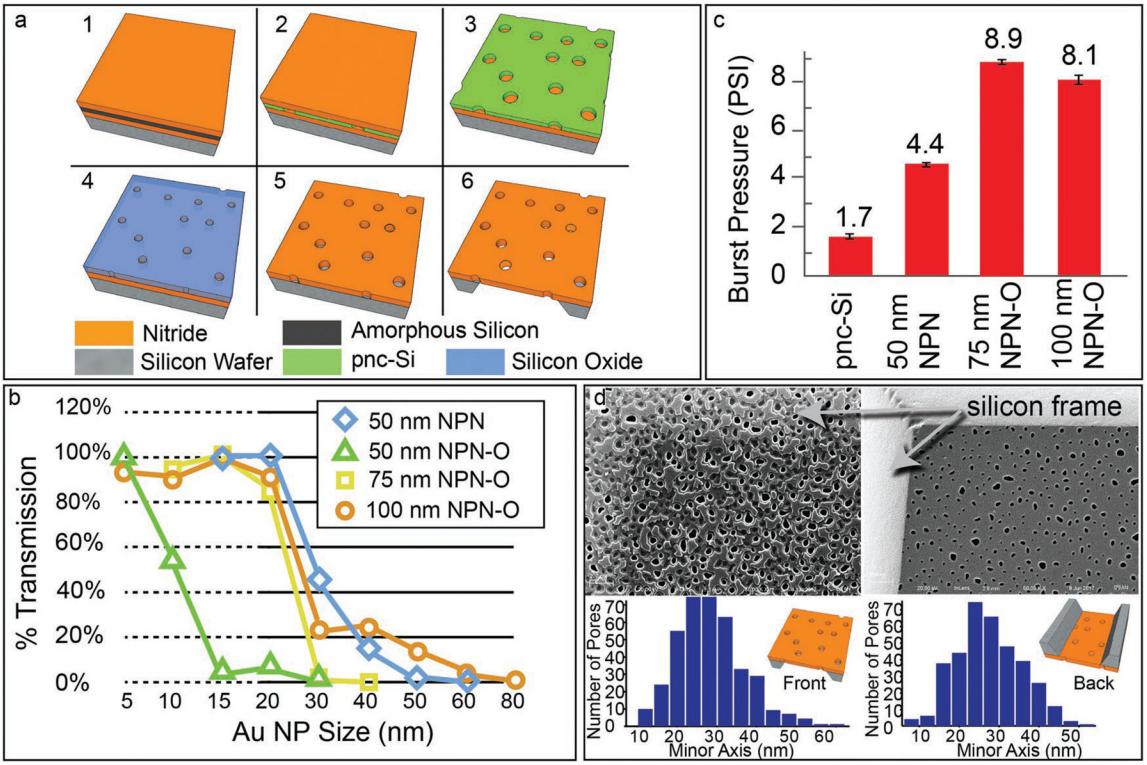

Figure 1.

Characterization of NPN-O. a) Process flow and structure for NPN-O membrane chips. 1) Silicon is deposited on wafers coated with 50, 75, or 100 nm of silicon nitride and 2) converted to 30 nm or 50 nm porous-nanocrystalline silicon (pnc-Si) by rapid thermal anneal. 3) Capping layer of nitride removed in etch. 4) The pnc-Si is oxidized to make it thicker and more resistive as an etch mask. 5) Pores are then transferred to SiN through a reactive ion etch (RIE) with also consumes the oxide mask. 6) A backside wet-etch is then performed to create membranes. b) Sieving Curves. Gold nanoparticle sieving curves show a ≈24 nm cutoff for 75 nm NPN-O with <10 nm resolution. A similar curve is seen for 100 nm NPN O but with a broad tail for large pore sizes. This tail is consistent with the creation of large pores from mergers of smaller pores during the longer RIE process. c) Burst Pressures. NPN-O is almost twice as strong as standard (50 nm) NPN, and five times stronger than pnc-Si. Surprisingly 100 nm NPN-O is not stronger than the 75 nm, possibly because of its higher porosity. d) Characterization by SEM. SEM images of both sides of a single 75 nm NPN-O membrane. The front side shows larger pores and thin patches of Si oxynitride patches as a byproduct of the oxidation step. The backside shows pristine SiN and smaller pores, which determine the selective properties of NPN-O. Reproduced with permission.[24] Copyright 2018, IEEE.

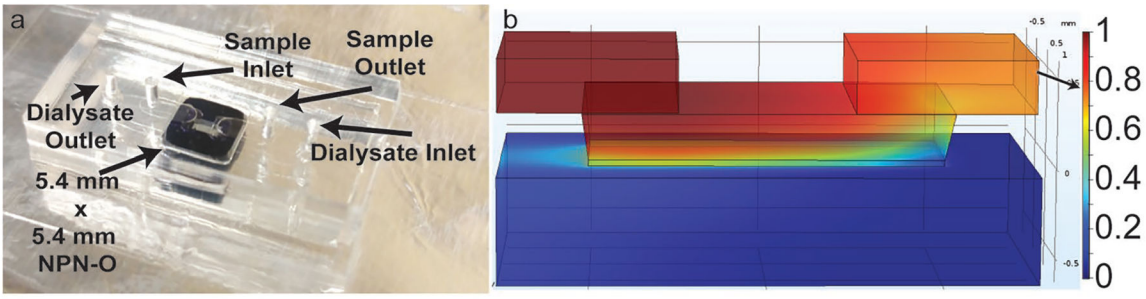

Figure 2.

Clearance data and hemocompatibility. a) Images of membrane chip and counter-flow device. b) COMSOL model showing the concentration of urea in the sample fluid in the channels above and below the dialysis chip and in the membrane itself (membrane thickness not shown to scale). Sample fluid (exiting at top right) shows concentration with reduction of >20%.

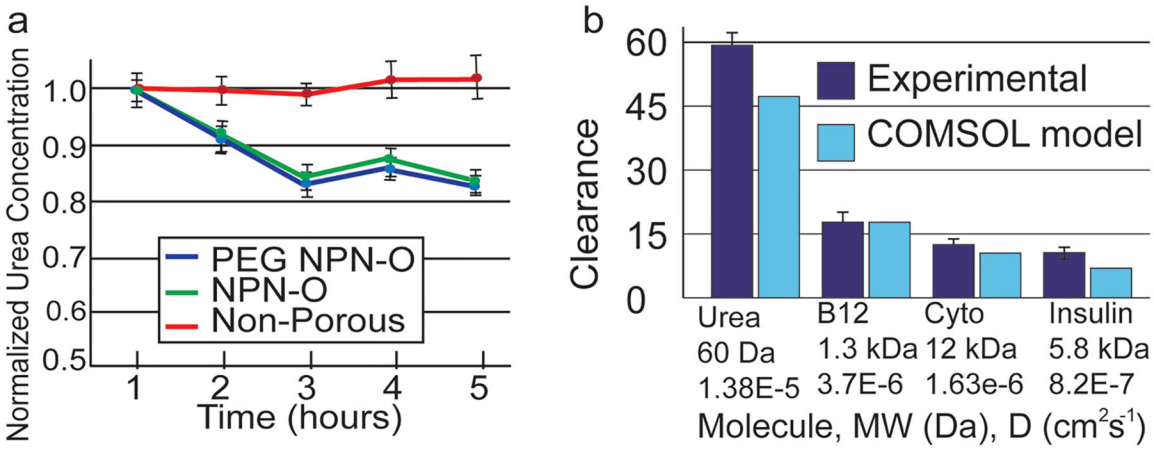

Figure 3.

Single-pass clearance data and static microdialysis results a) Single-pass urea clearance on single-membrane dialysis device (610 μm analyte channels). Protein fouling by serum is evaluated over dialysis window by measuring urea clearance in a single-pass over the membrane in a background of 100% serum. NPN-O and PEG-NPN-O showed a steady and almost identical 20% reduction in urea, while a nonporous control shows no reduction in urea concentration. b) Single-pass clearance with optimized two-membrane device (310 μm analyte channels). The two separate values of urea clearance are accounted for by the differences in the devices and flow rates used. Clearance decreases as the diffusion coefficients decrease (D_{urea} = 1.38E-5,[47] D_{B12} = 3.7E-6,[48] D_{Cyto} = 1.63E-6,[26] DInsulin = 8.2E-7[25]). Results are closely predicted by COMSOL model.

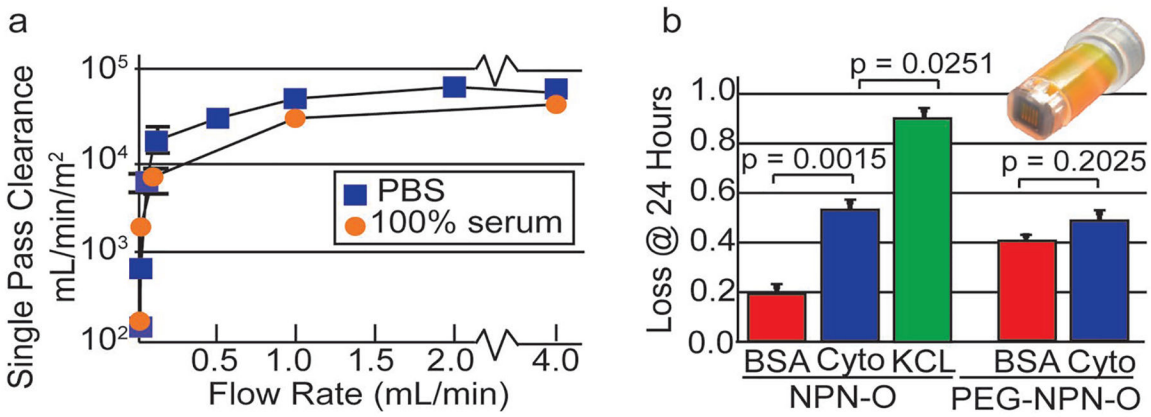

Figure 4.

Single-pass clearance data and static microdialysis results a) Single-pass clearance, normalized to the membrane surface area. b) Separation of middleweight proteins from albumin. Microdialysis experiments were performed over 24 h to evaluate the ability of coated and uncoated membranes to discriminate between BSA and cytochrome. Adsorption onto the surfaces of nonporous membranes and the spin cups were subtracted from the raw experimental data.

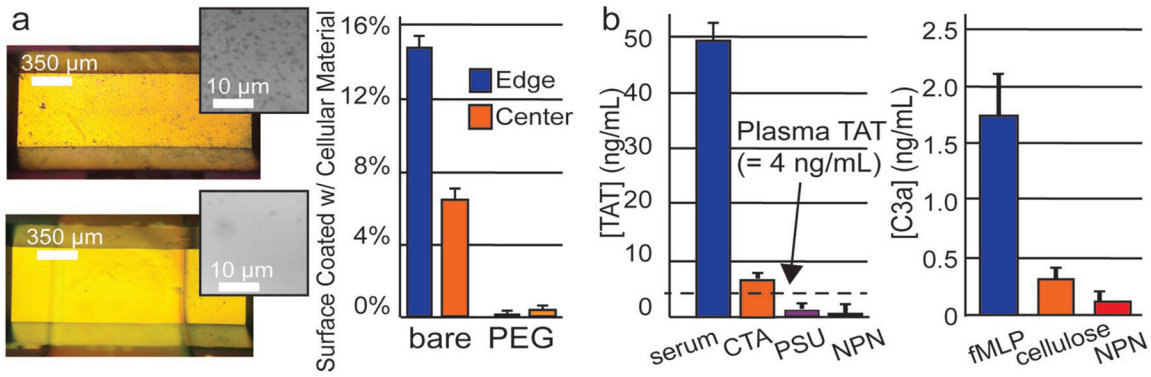

Figure 5.

Hemocompatibility a) Cellular adhesion with whole ovine blood in counter-flow device, comparing untreated versus PEG coated. Graph shows a 97% reduction in adhesion. b) Substrate Hemocompatibility Assessment. Coagulation assessed in term of TAT generation. Serum with 10×10^{-9} M fMLP, is used for the positive control. Immune activation presented in terms of C3a complement production. Whole blood with 10×10^{-9} M fMLP is used for the positive control. Sample size: $n = 3$ for all substrates.

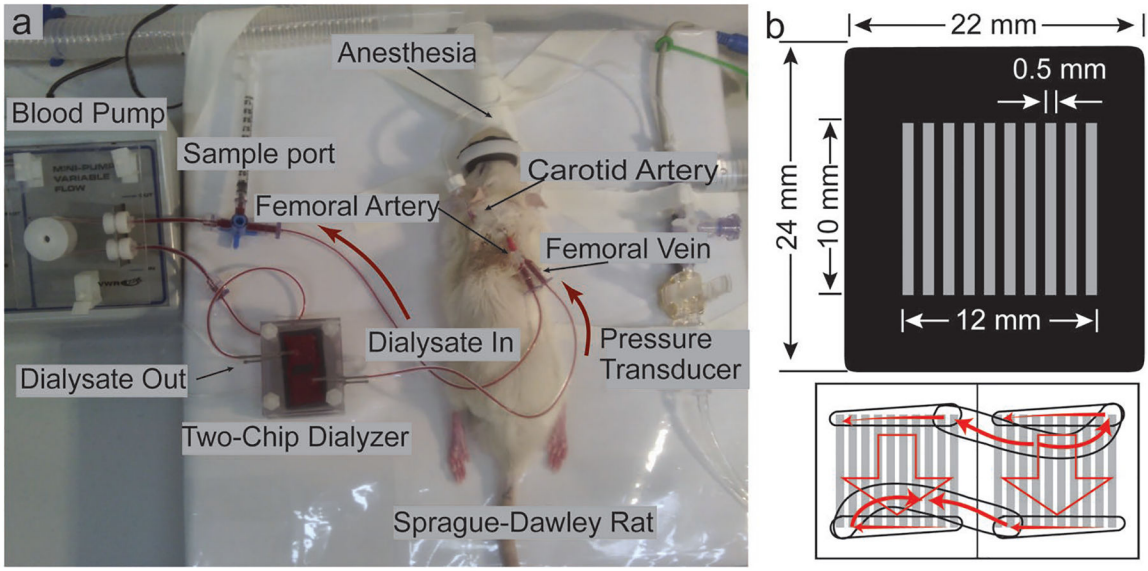

Figure 6.

Small animal study setup with NPN-O membrane chips. a) Sprague-Dawley rat (ex-breeder male) during a 4 h HD session using a two-chip dialyzer. b) NPN-O membrane chip layout and two-chip device blood path.

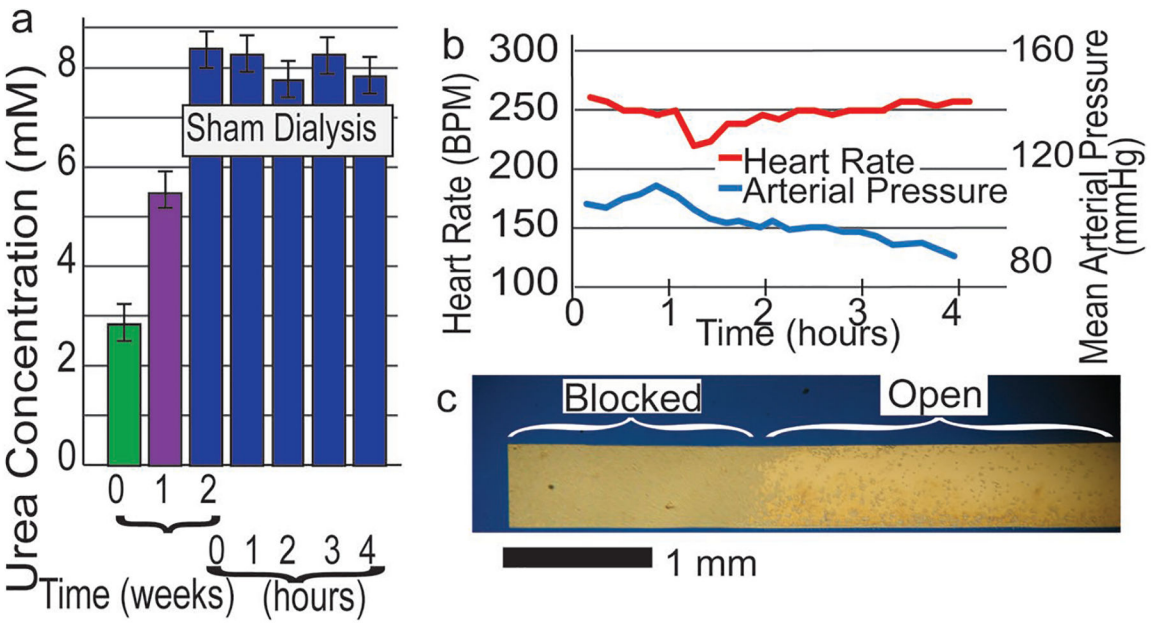

Figure 7.

Small animal study: uremia, sham dialysis, animal health, and adhesion. a) Rats fed an adenine containing diet showed increased serum urea levels after two weeks. Sham hemodialysis had no effect on serum urea. b) Heart rate and blood pressure recorded during a 4 h dialysis session. Decrease in arterial pressure indicates a deeper state of anesthesia and is well within expected range. c) Hemocompatibility, ≈10% reduction of membrane area due to cellular adhesion, post 4 h HD.

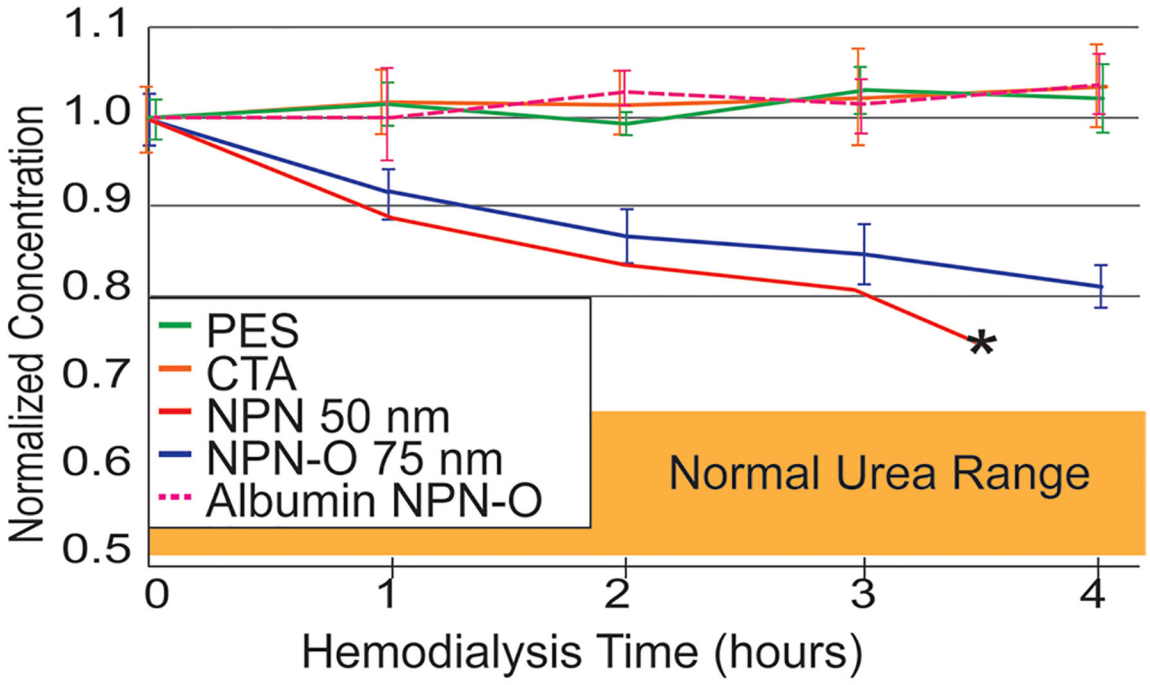

Figure 8.

Small animal study results with NPN-O membrane chips. Dialysis with commercial hemodialysis-membrane materials (PSU and CTA) shows no reduction in serum urea after 4 h of dialysis. Both 50 nm NPN membranes (in red) and 75 nm NPN-O membranes (in blue) show a significant decrease in serum urea in the rat animal model. Albumin is retained with both NPN and NPN-O. Note: The 50 nm NPN membrane failed after 3.5 h but the more robust 75 nm NPN-O membrane did not. Error bars show standard deviation.